

Ordering Topological Descriptors

Brittany Terese Fasy  *†

David L. Millman  †‡

Anna Schenfish  §

Abstract

Recent developments in shape reconstruction and comparison call for the use of many different types of topological descriptors (persistence diagrams, Euler characteristic functions, etc.). We establish a framework that allows for quantitative comparisons of topological descriptor types and therefore may be used as a tool in more rigorously justifying choices made in applications. We then use this framework to partially order a set of six common topological descriptor types. In particular, the resulting poset gives insight into the advantages of using verbose rather than concise topological descriptors. We then provide lower bounds on the size of sets of descriptors that are complete discrete invariants of simplicial complexes, both tight and worst case. This work sets up a rigorous theory that allows for future comparisons and analysis of topological descriptor types.

1 Introduction

The persistent homology transform and Euler characteristic transform of a shape in Euclidean space were first explored in [1], which shows the uncountable set of persistence diagrams (or Euler characteristic functions, respectively) corresponding to lower-star filtrations in every possible direction uniquely represents the underlying shape. That is, the uncountable collection of topological descriptors is *faithful* for the underlying shape. In practice, of course, any application can only make use of finite sets, which, unlike the infinite sets of [1], are not guaranteed to be faithful. This motivated theoretical work focused on finding finite faithful sets of descriptors [2–5].

The theoretical foundations regarding faithful sets of directional topological descriptors supports their use in shape comparison applications. A wide range of types of topological descriptors have been used in shape comparison applications, such as versions of persistence diagrams [6–11], versions of Euler characteristic functions [12–18], Betti functions [19–24], and other descriptors [25–27].

Thus, shape comparison by directional topological descriptors is an active area of applications research, and many different types of topological descriptors are used as tools in such work. Being able to faithfully represent a shape with a small number of descriptors is a desirable property for computational and storage reasons. How, then, should investigators choose the particular topological descriptor type to use in applications? While the computational complexities of computing each topological descriptor type is well studied, it is not yet clear to what extent the use of particular descriptor types impacts the minimum size of a faithful set. This uncertainty motivates our main question – *how can we rigorously compare topological descriptors in terms of their ability to uniquely correspond to shapes?*

First, we define relations for comparing general topological descriptors via their *strength equivalence classes*. We then focus on partially ordering the strength classes of a set of six popular descriptor types. This includes a strict inequality that separates the subset of verbose descriptor strength classes (see Figure 1). Finally, we provide lower bounds on the cardinality of representative sets for both concise and verbose descriptors. This includes constructions of simplicial complexes that require surprisingly large faithful sets. The constructions give us lower bounds that strongly indicate concise descriptors are generally much weaker than verbose descriptors, suggesting applications research may benefit from the use of verbose descriptors instead of the more widely adopted concise descriptors. This work sets up a rigorous theory that paves the pathway for future comparisons and analysis of topological descriptors.

*Depart. of Mathematical Sciences, Montana State U.

†School of Computing, Montana State U.

‡Blocky Inc.

§Corresponding author, Depart. of Mathematics and Computer Science, Eindhoven U. of Technology
brittany.fasy@montana.edu, david@blocky.rocks, a.k.schenfish@tue.nl

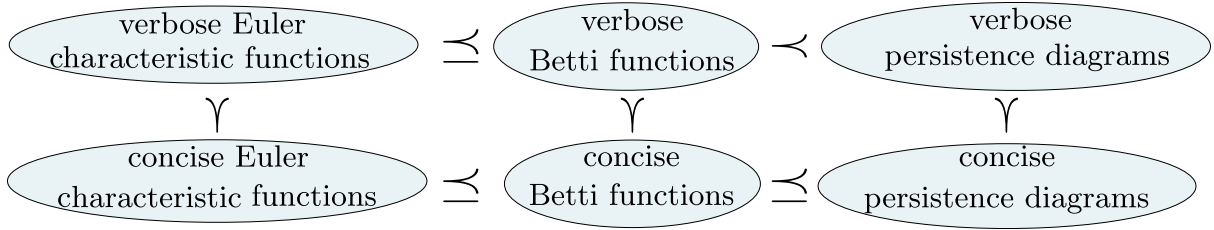


Figure 1: Summary of the relations between common descriptor types. The symbols \preceq and \prec denote weaker and strictly weaker, respectively. For example, concise persistence diagrams are always at least as efficient as concise Betti functions at forming faithful sets, where efficiency is measured by cardinality of faithful sets. That is, concise Betti functions are *weaker* than concise persistence diagrams.

2 Preliminary Considerations

We assume the reader has familiarity with ideas from topology, including homology, Betti numbers, and the Euler characteristic. See [28, 29] for further details. We always take \mathbb{N} to include zero. We write e_i to denote the i th unit standard basis vector. For a simplicial complex K , we use the notation K_i for its i -skeleton and n_i as the number of i -simplices. We always assume our simplicial complexes are finite. Furthermore, we assume our simplicial complexes are *geometric*, meaning each i -simplex is geometrically realized as the convex hull of $i + 1$ points in Euclidean space. A *filter* of K is a map $f: K \rightarrow \mathbb{R}$ such that, for $\tau, \sigma \in K$, if τ is a face of σ , then $f(\tau) \leq f(\sigma)$. Then, letting $F(t) := f^{-1}(-\infty, t]$, the sequence $\{F(t)\}_{t \in \mathbb{R}}$ is the *filtration* associated to f ; in particular, the filtration is a sequence of nested subcomplexes along with inclusion maps $F(i) \hookrightarrow F(j)$ for every $i \leq j$. Moreover, for each $k \in \mathbb{N}$, the inclusion $F(i) \hookrightarrow F(j)$ induces a linear map on homology, $H_k(F(i)) \rightarrow H_k(F(j))$. We write $\beta_k^{i,j}(K, f)$ to mean rank of this map, or simply $\beta_k^{i,j}$ if K and f are clear from context.

In particular, the *lower-star filter* of a simplicial complex K immersed in \mathbb{R}^d with respect to some direction $s \in \mathbb{S}^{d-1}$, is the map $f_s: K \rightarrow \mathbb{R}$ defined by $f_s(\sigma) = \max\{s \cdot v \mid v \in K_0 \cap \sigma\}$, where $s \cdot v$ denotes the dot product, and so is the height of v in direction s . Note that s defines a preorder on K_0 , $v_0 \leq v_1 \leq \dots \leq v_{n_0-1}$. Then the *lower-star filtration* of K with respect to s is

$$\emptyset \subset f_s^{-1}(-\infty, s \cdot v_0] \subseteq f_s^{-1}(-\infty, s \cdot v_1] \subseteq \dots \subseteq f_s^{-1}(-\infty, s \cdot v_{n_0-1}] = K.$$

Any filter function has *compatible index filters*, which are functions $f': K \rightarrow \mathbb{R}$ such that f' totally orders all the simplices of K and if $f(\tau) \leq f(\sigma)$, then $f'(\tau) \leq f'(\sigma)$. We say their corresponding filtrations are *compatible index filtrations*.

Since we define relations based on the ability of descriptor types to represent particular filtrations of simplicial complexes, we take the following definition.

Definition 1 (Topological Descriptor Type). *A topological descriptor type is a map whose domain is the collection of finite filtered geometric simplicial complexes. Given such a topological descriptor type, D , a single topological descriptor of type D is simply the image of a specific finite filtered geometric simplicial complex under D . We may often refer to a single topological descriptor simply as a descriptor.*

When considering many different filtrations of the same simplicial complex, we may index the filtrations by some parameter set, P . If a descriptor of type D corresponds to a filtration of a simplicial complex K where the filtration is parameterized by $p \in P$, we use the notation $D(K, p)$, or $D(p)$ when K is clear from context. Furthermore, we refer to the set of descriptors parameterized by P as $D(K, P) = \{p, D(K, p)\}_{p \in P}$. We use P for an arbitrary parameter set and S when the parameter set is specifically a subset of the sphere of directions.

We compare descriptor types by quantifying the number of descriptors needed to fully represent a shape. Specifically, we say a set of descriptors is *faithful* for a simplicial complex K if only K could have generated that same set of descriptors.

Definition 2 (Faithful Set). *Let K be a finite geometric simplicial complex and let P parameterize a set of filtrations of K . Let D be a topological descriptor type. We say that $D(K, P)$ is faithful if, for any finite geometric simplicial complex K' we have the equality $D(K', P) = D(K, P)$ if and only if $K' = K$.*

Next, we provide a reformulation of Definition 2 in terms of set intersections.

Lemma 1 (Sufficient and Necessary Condition for Faithfulness). *Let K be a simplicial complex, D a topological descriptor type, and P a set of parameters indexing the set $D(K, P)$. Then the set $D(K, P)$ is faithful if and only if*

$$\bigcap_{p \in P} \{K' \subset \mathbb{R}^d \mid D(K', p) = D(K, p)\} = \{K\}.$$

Proof. First, suppose that $D(K, P)$ is faithful. It is immediate that the intersection contains at least K . Suppose, towards a contradiction, that the intersection contains some $K' \neq K$. Then, for all $p \in P$, we have $D(K', p) = D(K, p)$, meaning that $D(K', P) = D(K, P)$, contradicting the faithfulness of $D(K, P)$.

Next, suppose that the intersection only contains K . This means there is no $K' \neq K$ such that we have equality $D(K', p) = D(K, p)$ for all $p \in P$, i.e., there is no $K' \neq K$ such that $D(K', P) = D(K, P)$, so we see that $D(K, P)$ is faithful. \square

The definition of Lemma 1 allows us to state the following lemma about finiteness of a faithful set. In particular, we show if a descriptor type has a finite faithful set for the vertex set of a complex, the minimum faithful set for the entire complex is also finite.

Lemma 2 (Sufficient Conditions for Finite Faithful Set). *Let $K \in \mathbb{R}^d$ be a finite simplicial complex and let D be a type of topological descriptor that can faithfully represent K . Suppose there exists a set of descriptors of type D that is faithful for K_0 with finite cardinality. Then there exists a finite faithful set of type D for K .*

Proof. From the hypotheses, we know there is a finite set $D(K, P_0)$ that is faithful for K_0 and a set $D(K, P)$ that is faithful for K . Since $D(K, P)$ is faithful for K , we have

$$\bigcap_{p \in P} \{K' \subset \mathbb{R}^d \mid D(K', p) = D(K, p)\} = \{K\}. \quad (1)$$

Similarly, since $D(K, P_0)$ is faithful for K_0 , we define

$$B := \bigcap_{p \in P_0} \{K' \subset \mathbb{R}^d \mid D(K', p) = D(K, p)\}$$

and see that $B \subseteq \{K' \mid K'_0 = K_0\}$, i.e., B is a subset of all simplicial complexes built out of the vertices of K . In particular, we note that this set is finite; since $|K_0| = n_0$ is finite, there are a finite number of simplicial complexes we can build over this set of vertices.

Suppose there is some $K^1 \in B$ such that $K^1 \neq K$ (if not, and the intersection is only K , then $D(K, P_0)$ is a faithful set for K , and since P_0 is finite by assumption, we are done). Then there must be some parameter $p^1 \in P$ for which we have $K^1 \notin \{K' \in \mathbb{R}^d \mid D(K', p) = D(K, p)\}$. Otherwise, the intersection in Equation (1) would contain K^1 in addition to just K , so by Lemma 1, $D(K, P)$ would not be faithful.

Since B is a finite set, there are finite $K^i \neq K$ contained in B , and by similar reasoning, for each such K^i we can find a direction $p^i \in P$ whose set of possible complexes does not include K^i . Denote the number of complexes not equal to K that are contained in B by n . Then the set $P_* = P_0 \cup \{p^1, p^2, \dots, p^n\}$ is finite, and $D(K, P_*)$ faithfully represents K . \square

3 Six Common Descriptor Types

The set we partially order is the strength equivalence classes of six popular topological descriptor types, which we define here. We begin with concise persistence diagrams.

Definition 3 (Concise Persistence Diagram, ρ). *Let $f : K \rightarrow \mathbb{R}$ be a filter function. We define the k th-dimensional persistence diagram as the following multiset:*

$$\rho_k^f := \left\{ (i, j)^{\mu^{(i, j)}} \text{ s.t. } (i, j) \in \overline{\mathbb{R}}^2 \text{ and } \mu^{(i, j)} = \beta_k^{i, j-1} - \beta_k^{i, j} - \beta_k^{i-1, j-1} + \beta_k^{i-1, j} \right\},$$

where $\overline{\mathbb{R}} = \mathbb{R} \cup \{\pm\infty\}$ and $(i, j)^m$ denotes m copies of the point (i, j) . The concise persistence diagram of f , denoted ρ^f , is the union of all k -dimensional concise persistence diagrams $\rho_k^f := \cup_{k \in \mathbb{N}} \rho_k^f$.

Since simplices can appear at the same parameter value in a general filtration, not all cycles are represented in the persistence diagram. However, having every simplex “appear” in a topological descriptor is helpful, in addition to being natural. Thus, we introduce *verbose* descriptors, which contain this information. We begin with *verbose persistence diagrams*:

Definition 4 (Verbose Persistence Diagram, $\hat{\rho}$). Let $f : K \rightarrow \mathbb{R}$ be a filter for K , and let f' be a compatible index filter. For $k \in \mathbb{N}$, the k -dimensional verbose persistence diagram is the following multiset:

$$\hat{\rho}_k^f := \left\{ (f(\sigma_i), f(\sigma_j)) \mid (i, j) \in \rho_k^{f'} \right\}. \quad (2)$$

The verbose persistence diagram of f , denoted $\hat{\rho}^f$, is the union of all $\hat{\rho}_k^f$.

Recording invariants other than homology throughout a filtration leads to other topological descriptor types; recording Betti numbers gives us *Betti functions*.

Definition 5 (Concise and Verbose Betti Functions, β and $\hat{\beta}$). Let $f : K \rightarrow \mathbb{R}$ be a filter function. The k th Betti function is the function $\beta_k^f : \mathbb{R} \rightarrow \mathbb{Z}$ defined by

$$\beta_k^f(t) := \beta_k(f^{-1}(-\infty, t]).$$

The collection of Betti functions for all dimensions, $\beta^f := \{\beta_k^f \mid k \in \mathbb{N}\}$, is known as the Betti function, and is written as simply β when f is clear from context.

Let f' be an index filter compatible with f . We call $\sigma \in K$ positive (respectively, negative) for β_k if the inclusion of σ into the index filtration associated to f' increases (respectively, decreases) β_k . We denote the positive (negative) simplices by L_k^+ (and L_k^-). Then the k th verbose Betti function is the function $\hat{\beta}_k^f : \mathbb{R} \rightarrow \mathbb{Z}^2$ defined by

$$\hat{\beta}_k^f(p) := \left(|\{\sigma \in L_k^+ \mid f(\sigma) \leq p\}|, |\{\sigma \in L_{k+1}^- \mid f(\sigma) \leq p\}| \right).$$

The collection of verbose Betti number functions for each dimension is known as the verbose Betti function and is denoted $\hat{\beta}$. Again, we omit the superscript f when it is clear from context.

If we record Euler characteristic in a filtration, we obtain Euler characteristic functions.¹

Definition 6 (Concise and Verbose Euler Characteristic Functions, χ and $\hat{\chi}$). Let $f : K \rightarrow \mathbb{R}$ be a filter function. The Euler characteristic function is the function $\chi^f : \mathbb{R} \rightarrow \mathbb{Z}$ defined by mapping $p \in \mathbb{R}$ to the Euler characteristic of $\{f^{-1}(-\infty, p]\}$:

$$\chi^f(p) := \chi(\{f^{-1}(-\infty, p]\}).$$

Let f' be an index filter compatible with f . We call $\sigma \in K$ even (respectively, odd) if the dimension of σ is even (respectively, odd). We denote the set of even (odd) simplices by E (and O). Then the verbose Euler characteristic function for f is the function $\hat{\chi}^f : \mathbb{R} \rightarrow \mathbb{Z}^2$ defined by

$$\hat{\chi}^f(p) = (|\sigma \in E \text{ s.t. } f(\sigma) \leq p|, |\sigma \in O \text{ s.t. } f(\sigma) \leq p|).$$

In other words, $\hat{\chi}$ represents χ as a parameterized count of even- and odd-dimensional simplices. We omit the superscript f when it is clear from context.

See Figure 2 for an example of each descriptor. Although descriptors of the above types may arise from any type of filtration (or indeed, even from abstract one-parameter persistence modules), since we compare the ability of the above descriptors to represent shapes, we consider them only as corresponding to a lower-star filtration of a finite simplicial complex.

While concise descriptors may feel more familiar, the idea of verbose descriptors is not new. Indeed, many typical algorithms for computing persistence (e.g., [29, Chapter VII]), explicitly compute topological events with trivial lifespan but then discard them from the output. In [30], persistence diagrams are the same as our definition of $\hat{\rho}$. Verbose descriptors are closely connected to the charge-preserving morphisms of [31, 32]. In [33], verbose persistence is defined via filtered chain complexes; [34–37] also take this view as a foundational definition. The relevance of using verbose versus concise descriptors was explored in [36, 38, 39], although with slightly different language.

Verbose (concise) descriptors are sometimes called augmented (non-augmented, respectively) in the literature. Furthermore, we refer to points on a verbose diagram with zero-lifespan (i.e., points on the diagonal) as *instantaneous*. Such points correspond to length-zero barcodes in a verbose barcode, which are sometimes referred to as *ephemeral*.

While we chose the six descriptor types above due to their relevance in applications, we emphasize that Definition 1 allows for much greater generality than presented in this section. We explore a few non-standard descriptor types in Appendix A.

¹Euler characteristic functions and Betti functions are sometimes called Euler (characteristic) curves or Betti curves, respectively.

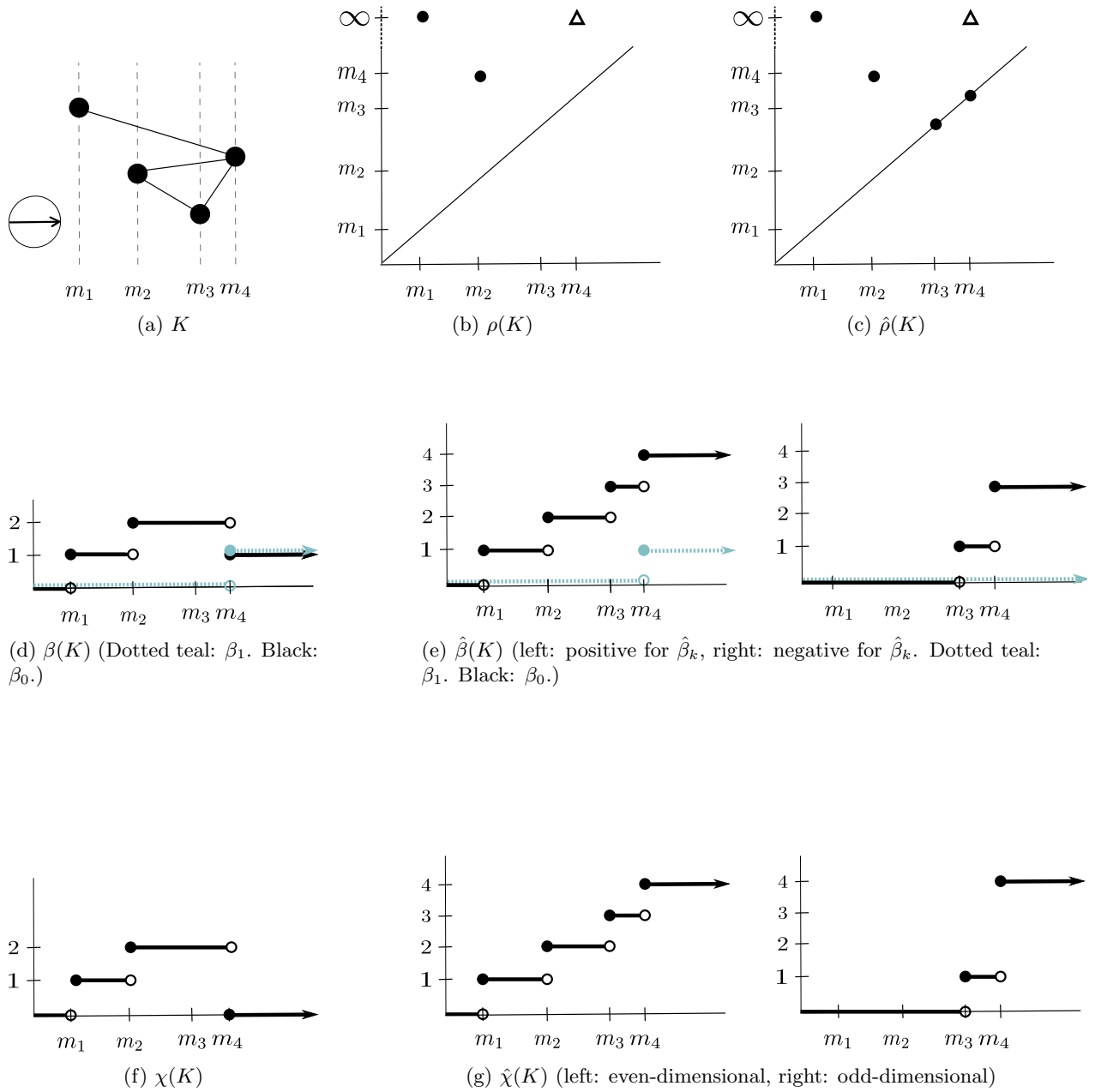


Figure 2: Six descriptors corresponding to the lower-star filtration in the direction indicated by the arrow of the simplicial complex in (a).

4 Relating Descriptor Types

We now develop tools to compare topological descriptor types, and do so by comparing the cardinalities of faithful sets. Since $|D(K, P)| = |P|$, we use the notation $|P|$ for brevity when discussing the cardinality of a set $D(K, P)$. In what follows, we restrict our attention to indexing sets that are finite, countably infinite, or uncountably infinite.

Intuitively, descriptor types that are not able to form faithful sets should be *weaker* than those that can, descriptor types that require uncountably infinite sets in order to achieve faithfulness should be considered as weaker than those that can construct faithful sets from a countably infinite set of descriptors, and descriptor types that require (countable or uncountable) infinite sets should be weaker than those whose minimum faithful sets are finite. Thus, we want our definition to have a sort of inverse relationship, where large cardinalities correspond to weaker descriptor types. We use the notation \aleph_0 to denote the cardinality of \mathbb{N} , and \aleph_1 to denote the cardinality of \mathbb{R} . By the axiom of choice, we can compare these cardinalities, $\aleph_0 < \aleph_1$; see, e.g., [40, Ch. 2].

How then, should we think of the “cardinality” of a faithful set when no faithful set exists? Declaring it to be zero would have the opposite desired effect, since then descriptor types unable to form faithful sets would be placed at the wrong end of our intuitive order. In order to cleanly discuss relations when considering descriptor type and simplicial complex pairings for which there are *no* faithful sets, we consider any infimum taken over the empty set to have cardinality \aleph_\top , which we consider as strictly greater than any cardinality (in particular, \aleph_1). This is done simply so that situations where there are no faithful sets are recorded as “worse” than situations where there are infinite faithful sets.²

First, we define what it means to say two topological descriptor types have equal *strength*.

Definition 7 (Equal Strength). *Let A and B be topological descriptor types. If, for all simplicial complexes K ,*

$$\inf\{|P| \text{ s.t. } A(K, P) \text{ is faithful}\} = \inf\{|P| \text{ s.t. } B(K, P) \text{ is faithful}\},$$

then we say A and B have equal strength, denoted $[A] = [B]$.

In fact, this relation defines equivalence classes of strength.

Lemma 3 (Equivalence Relation). *The relation $=$ is an equivalence relation.*

Proof. When we compare sizes of faithful sets, we are comparing values in the set $\mathbb{N} \cup \{\aleph_0, \aleph_1, \aleph_\top\}$. Since equality of values in this set is reflexive, symmetric, and transitive, it follows that the relation given in Definition 7 is also reflexive, symmetric, and transitive. \square

As an example, consider the topological descriptor denoted $-\rho$ that takes a lower-star filtration in direction s , and produces $\rho(-s)$, the persistence diagram in direction $-s$. Although generally we have $\rho(s) \neq \rho(-s)$ (as multisets), we observe that a faithful set $\rho(K, S)$ has the same cardinality as the faithful set $-\rho(K, -S)$, and if a simplicial complex has no faithful set of type ρ , then it has no faithful set of type $-\rho$. Thus, $[\rho] = [-\rho]$.

Next, we define what it means for the strength class of a topological descriptor type to be *weaker* than another, and show this is indeed a well-defined ordering relation.

Definition 8 (Relation \preceq). *Let A and B be two topological descriptor types. Suppose that, for every simplicial complex K :*

$$\inf\{|P| \text{ s.t. } A(K, P) \text{ is faithful}\} \geq \inf\{|P| \text{ s.t. } B(K, P) \text{ is faithful}\}.$$

Then we say the class of A is weaker than the class of B , denoted $[A] \preceq [B]$.

Lemma 4. *The relation \preceq is well-defined on sets of strength equivalence classes.*

Proof. When we compare sizes of faithful sets, we are comparing values in $\mathbb{N} \cup \{\aleph_0, \aleph_1, \aleph_\top\}$. Since the relation \leq on values in this set is reflexive, antisymmetric, and transitive, it follows that the relation given in Definition 8 is also reflexive, antisymmetric, and transitive. \square

²We hope any discomfort caused by our use of \aleph_\top will be outweighed by the benefit of being able to avoid awkward case analyses.

We may encounter strength classes related by \preceq that are not equal. That is, the class of A is *strictly weaker than* the class of B (denoted $[A] \prec [B]$) if $[A] \preceq [B]$ and $[A] \neq [B]$. That is, if $[A] \preceq [B]$ and there exists a simplicial complex for which the minimum faithful set of type B is strictly smaller than that of type A , or for which there exists a faithful set of type B but not of type A . We note that general descriptor types need not be comparable; see Lemma 15 of Appendix A.

Now that we have a way of ordering (comparable) descriptor classes, we are ready to discuss determining ordering. It is often difficult to directly determine and compare minimal faithful sets in general, so it is useful to have a variety of tools that allow us to determine how descriptors are related. We conclude this section by defining reduction of one descriptor to another, and show this is another valid strategy for determining equivalence class order.

Definition 9 (Reducing a Descriptor to Another). *Let A and B be two topological descriptor types, let P be a family of filtration parameters, and let K be a simplicial complex. We say B is reducible to A if there exists an algorithm such that, for each $p \in P$, the input of $B(K, p)$ into the algorithm produces the output $A(K, p)$.*

An alternate way to frame the preceding definition is as a universal property, where B is reducible to A if A factors through B , for all inputs of filtered simplicial complexes. Figure 3 shows this factorization for a single filtered simplicial complex. Intuitively, if B is reducible to A , a descriptor $B(K, p)$ has all

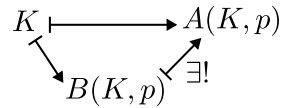


Figure 3: Reduction from B to A viewed diagrammatically, for a specific simplicial complex K and parameter p . If B is reducible to A , such a diagram exists for all choices of K and p .

the information needed to obtain $A(K, p)$, i.e., B is at least as informative as A , and possibly more so. More formally, we have the following lemma:

Lemma 5. *Let A and B be two topological descriptor types. If B is reducible to A , we have $[A] \preceq [B]$.*

Proof. Let K be a simplicial complex. Then, we define the sets $W_A := \{P \text{ s.t. } A(K, P) \text{ is faithful}\}$ and $W_B := \{P \text{ s.t. } B(K, P) \text{ is faithful}\}$. Since B is reducible to A , we know that for each $P \in W_A$, we also have $P \in W_B$. Hence, $W_A \subseteq W_B$. Note that these sets are what index the infimums in Definition 8 and so, we have $[A] \preceq [B]$. \square

5 A Proof of Partial Order

In this section, we prove our main theorem, a partial order on the six topological descriptors of Section 3. While the results and definitions of previous sections were phrased generally, we now specifically focus on descriptors corresponding to lower-star filtrations of a simplicial complex. First, we state our general position assumption.

Assumption 1 (General Position). *We say a simplicial complex K in \mathbb{R}^d is in general position if, for all k with $1 \leq k \leq d + 1$, every subset of K_0 of size k is affinely independent.*

Note that without this assumption, relating concise descriptors becomes trivial; see Lemma 16 of Appendix A. Thus, we proceed assuming general position, and see a more interesting order of concise descriptor types; verbose descriptors are similarly ordered.

Lemma 6. $[\chi] \preceq [\beta] \preceq [\rho]$ and $[\hat{\chi}] \preceq [\hat{\beta}] \preceq [\hat{\rho}]$.

Proof. The proof follows directly from a reduction argument. We can reduce any $\rho(s)$ to $\beta(s)$ by “forgetting” the relationship between birth and death events. We can then reduce $\beta(s)$ to $\chi(s)$ by taking the alternating sum of points from $\beta(s)$. A nearly identical argument shows the relationship between verbose versions of these descriptors. \square

The reduction from ρ to χ was also observed in [3, Prop 4.13]. We also use a reduction argument to order the classes of a concise descriptor type and its verbose counterpart.

Lemma 7. $[\chi] \preceq [\hat{\chi}]$, $[\beta] \preceq [\hat{\beta}]$, and $[\rho] \preceq [\hat{\rho}]$.

Proof. Each verbose descriptor has a clear reduction to its concise counterpart. A verbose persistence diagram becomes a concise persistence diagram by removing all on-diagonal points. Verbose Betti functions and verbose Euler characteristic functions become concise if we subtract their second coordinates from their first coordinates. Then by Lemma 5, we have the desired relations. \square

Next, we show no concise class is equal to a verbose class, i.e., the inequalities of Lemma 7 are strict.

Lemma 8. For $D \in \{\chi, \beta, \rho\}$ and $\hat{D} \in \{\hat{\chi}, \hat{\beta}, \hat{\rho}\}$, we have $[D] \neq [\hat{D}]$.

Proof. To show inequality of strength classes, we find a simplicial complex for which minimum faithful sets of type D and \hat{D} have different cardinalities. Let K be the simplicial complex that is a single edge in \mathbb{R}^2 with vertex coordinates $(1, 1)$ and $(1, 2)$. See Figure 4 for this complex, and an illustration for the specific case $\hat{D} = \hat{\rho}$. In the direction e_1 , if $\hat{D} = \hat{\rho}$, we see an instantaneous birth/death and an infinite birth in degree zero. If $\hat{D} = \hat{\beta}$, we see two positive simplices and one negative simplex for Betti zero. If $\hat{D} = \hat{\chi}$, we see two even simplices and one odd simplex. This all occurs at height 1, and, as there are no other events, which, is only explainable by the presence of a single edge. From $\hat{D}(e_2)$, we see a non-instantaneous and instantaneous event at heights 1 and 2, respectively, which give us the y -coordinates of our two vertices. Then K is the only complex that could have generated both $\hat{D}(e_1)$ and $\hat{D}(e_2)$, i.e., the set $\hat{D}(K, \{e_1, e_2\})$ is faithful.

Next, consider the descriptor type D . For any $s \in \mathbb{S}^1$, $D(s)$ contains exactly one event; if the lowest vertex of the edge with respect to s has height a in direction s , then $D(s)$ records a change in homology/Betti number/Euler characteristic at height a and records no other changes. Thus, $D(s)$ can only give us information about one coordinate of the vertex set of K at a time, corresponding to whichever vertex is lowest in direction s . However, K has three relevant coordinates; namely, $x = 1$, $y = 1$, and $y = 2$ meaning it is not possible for any faithful set of type D to have size less than three. Thus, since $3 \neq 2$, we have shown $[D] \neq [\hat{D}]$, as desired. \square

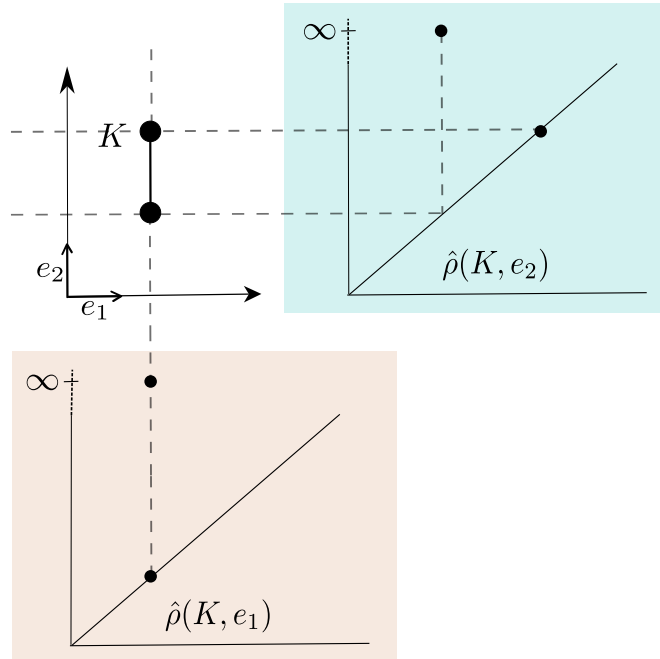


Figure 4: The simplicial complex considered in the proof of Lemma 8 as well as the verbose diagrams in directions e_1 and e_2 . Note that $\hat{\rho}(K, \{e_1, e_2\})$ is indeed a faithful set, since we can recover the coordinates of both vertices ($\hat{\rho}(K, e_1)$ tells us the x -coordinates and $\hat{\rho}(K, e_2)$ tells us the y -coordinates), as well as determine there is only a single edge present (there is only one instantaneous zero-dimensional point in each verbose diagram). The concise versions of these diagrams do not have on-diagonal points, and each only contain a single point at ∞ . This is true for concise diagrams corresponding to any direction.

The specific inequality $[\chi] \neq [\hat{\rho}]$ is also implied by [5, Thm. 10].

The fact that the sets of directions described in [4] form faithful sets of $\hat{\rho}$'s, $\hat{\beta}$'s, or $\hat{\chi}$'s with equal cardinality might make it seem as though our verbose descriptors are all in the same strength class. The

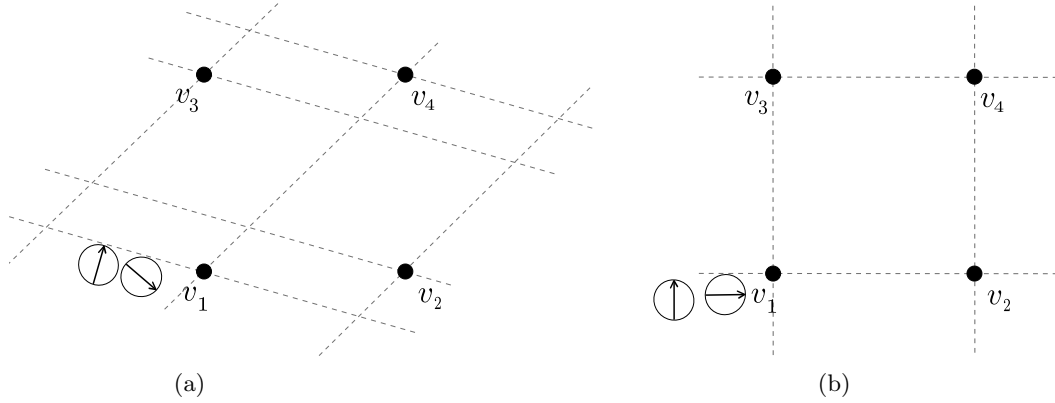


Figure 6: For four vertices on an axis-aligned grid, the heights of events from two filtrations in the indicated directions are shown as dashed grey lines. Although we know the number of vertices on each line, for two directions not both in $\{\pm e_1, \pm e_2\}$, as in (a), there are multiple vertex sets satisfying these constraints. Only when choosing one each of $\pm e_1$ and $\pm e_2$, as in (b), is the set of vertices satisfying these constraints unique.

Theorem 1 (Partial Ordering). *The following diagram is a correct partial order on strength classes of topological descriptors.*

$$\begin{array}{ccccc}
 [\hat{\chi}] & \xrightarrow{\preceq} & [\hat{\beta}] & \xrightarrow{\preceq} & [\hat{\rho}] \\
 \prec \uparrow & & \prec \uparrow & & \prec \uparrow \\
 [\chi] & \xrightarrow{\preceq} & [\beta] & \xrightarrow{\preceq} & [\rho]
 \end{array}$$

6 Bounds on Faithful Sets

This section provides lower bounds on the size of faithful sets of the six descriptor types of Section 3. Each subsection begins with a statement of tight lower bounds, but the more interesting results are finding examples of simplicial complexes whose minimal faithful set is large. Thus, the main theorems of this section provide lower bounds on the worst-case minimum size of faithful sets.

6.1 Concise Descriptor Bounds

A defining feature of concise descriptors is that there are not generally events at the height of every vertex in a filtration. Notably, the closer a feature becomes to colinear, coplanar, etc., the smaller the range of directions that can detect it becomes ([41, Sec. 4] explores this specifically for χ 's). Difficulty detecting the presence or absence of structures that are near to the same affine subspace puts greater restrictions on the ability of concise descriptors to form faithful sets. We use the following definition as a tool in making this claim precise.

Definition 10 (Simplex Envelope). *Let K be a simplicial complex in \mathbb{R}^d and let $\sigma \in K$. Let $S \subseteq \mathbb{S}^{d-1}$ be a set of directions. Then, we define the envelope of σ , denoted P_σ^S , as the intersection of (closed) supporting halfspaces*

$$P_\sigma^S = \bigcap_{s \in S} \{p \in \mathbb{R}^d \mid s \cdot p \geq \min_{v \in \sigma} (s \cdot v)\}.$$

If S is clear from context, we write P_σ . By the dimension of P_σ , we mean the largest dimension of ball that can be contained entirely in P_σ . By ∂P_σ , we mean the boundary of P_σ .

See Figure 7 for an example of a simplex envelope. Since P_σ^S is an intersection of convex regions, it is itself convex. Furthermore, since, with respect to each $s \in S$, the height of each point of σ is greater than or equal to its minimum vertex, we see that P_σ^S contains σ .

Remark 1. *Intersections of closed halfspaces is a well-studied phenomenon in convex geometry. The simplex envelopes of Definition 10 have connections to topics such as convex cones, support functions, etc. See [42, 43] for further information. In particular, [43, Thm 3.1.1, Cor 3.1.2] establish that a simplex envelope in the sense of Definition 10 with respect to the entire sphere of directions is the simplex itself.*

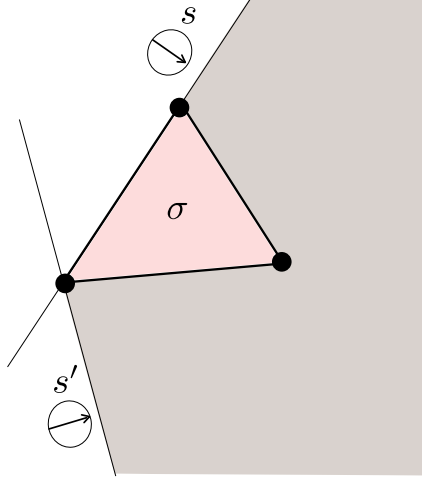


Figure 7: Given $S = \{s, s'\}$, the envelope for σ is the grey and pink shaded regions.

We use simplex envelopes to define a necessary condition for concise descriptors to form a faithful set for a simplicial complex.

Lemma 10 (Envelope Dimensions for Faithful Concise Sets). *Let K be a simplicial complex embedded in \mathbb{R}^d , let $D \in \{\chi, \beta, \rho\}$, and let $S \subseteq \mathbb{S}^{d-1}$ such that $D(K, S)$ faithful. Then, for any maximal simplex σ in K , the dimension of P_σ equals the dimension of σ .*

Proof. Let k denote the dimension of σ , and let c denote the dimension of P_σ . First, we observe that since σ is contained in P_σ , we must have $k \leq c$. The claim is trivial when $k = d$, so we proceed with the case $k < d$ and assume, by way of contradiction, that $k < c$.

We claim that in this case, 1) at every interior point of σ , there is a normal vector that ends in the interior of P_σ , and 2) letting p denote the endpoint of such a vector, p is higher than the lowest vertex of σ with respect to each $s \in S$.

The first part of the claim, 1), is true since otherwise, P_σ would be k -dimensional. 2) is true since each halfspace defining P_σ contains the lowest vertex (or vertices) of σ with respect to the corresponding direction. Thus, since p is in the interior of P_σ , it must be higher than this lowest vertex (or vertices) with respect to the corresponding direction.

Now consider the simplicial complex K' , defined as having all the simplices of K in addition to the simplex formed by taking the geometric join of p and σ , i.e., the simplex $p * \sigma$. We claim that, for any $s \in S$, we have $D(K', s) = D(K, s)$. First, we note that since $p * \sigma$ deformation retracts onto σ , K' has the same homology as K . Next, we observe that $D(K', s)$ and $D(K, s)$ cannot differ by more than a connected component birth/death; higher dimensional differences would require more than the join of a point with an existing face.

Finally, since p is higher than the lowest vertex of σ with respect to any direction $s \in S$, the simplex $p * \sigma \in K'$ does not correspond to any connected component birth or death in $D(K', s)$ that was not present in $D(K, s)$. Thus, we have shown $D(K', S) = D(K, S)$. This contradicts the assumption that $D(K, S)$ is faithful, so we must have $k = c$. \square

A simple extension of Lemma 10 gives the following.

Corollary 1 (Count of Concise Descriptors Per Maximal Simplex). *Let K be a simplicial complex in \mathbb{R}^d , let $D \in \{\chi, \beta, \rho\}$, and let $S \subseteq \mathbb{S}^{d-1}$. If $D(K, S)$ is faithful, then for each maximal simplex $\sigma \in K$ of dimension $k < d$, the set S has at least $d - k + 1$ directions perpendicular to σ . If $k < d - 1$, these directions are pairwise linearly independent with one another.*

Proof. Since $D(K, S)$ is faithful, we know by Lemma 10 that P_σ must be k -dimensional. Recall that P_σ is an intersection of closed half spaces. Then, for P_σ to be k -dimensional, it is a standard result in manifold theory that this intersection requires $d - k + 1$ hyperplanes, and if $k < d - 1$, these hyperplanes must not be parallel. The result follows. \square

The next corollary follows from both Lemma 10 and Corollary 1.

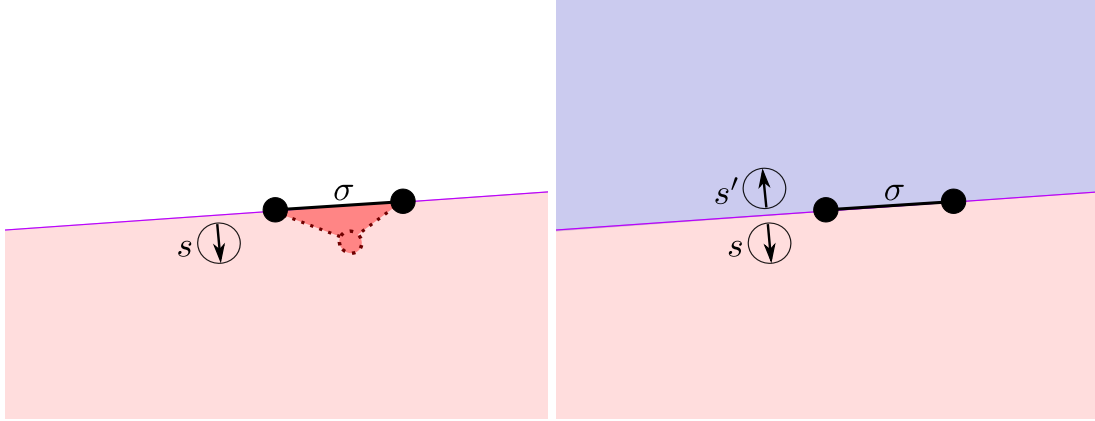


Figure 8: With only the single direction s perpendicular to maximal edge $\sigma \subset \mathbb{R}^2$, the envelope P_σ^s is two-dimensional, shown as the pink shaded halfspace in the left figure. Then, we could construct an adversarial two-simplex contained entirely in P_σ^s that is undetectable by $D(s)$, for $D \in \{\chi, \beta, \rho\}$. On the right, the inclusion of s' reduces $P_\sigma^{\{s,s'\}}$ to a linear subspace (shown as the purple intersection of pink and blue halfspaces) and the adversarial two-simplex would be detected by $D(s')$.

Corollary 2 (Tight Lower Bound). *Let K be a simplicial complex in \mathbb{R}^d , $D \in \{\chi, \beta, \rho\}$, and $S \subseteq \mathbb{S}^{d-1}$. Suppose that $D(K, S)$ is faithful. Then $|S| \geq d + 1$, and this bound is tight.*

This bound is met whenever K is (for example) a single vertex. However, the above bound is generally not met, and the minimum cardinality of a representative set of concise descriptors is generally much higher. In practice, the requirement that each maximal k -simplex in a simplicial complex corresponds to $d - k + 1$ perpendicular directions is a huge hindrance when forming faithful sets. Counteracting the need for perpendicular directions is the fact that, as d increases, more simplices span common hyperplanes, and thus perpendicular directions can increasingly be shared. The following organizes these observations into a more precise statement and construction bounding the worst case.

Theorem 2 (Lower Bound for Worst-Case Concise Descriptor Complexity). *Let $D \in \{\chi, \beta, \rho\}$ and let K be a simplicial complex in \mathbb{R}^d with n_1 edges. Then the worst-case cardinality of a minimal descriptor set of type D is $\Omega(d + n_1)$.*

Proof. We proceed by constructing a simplicial complex and bounding the minimum cardinality of a faithful set. Suppose, for $d > 2$, that K is a graph in \mathbb{R}^d comprised of $n_1 < d - 1$ edges, and suppose that, for some set of directions $S \subseteq \mathbb{S}^{d-1}$, $D(K, S)$ is a faithful set. Then by Lemma 10, the envelope of each maximal edge σ must be one-dimensional. Furthermore, by Corollary 1, for every such σ , S must contain $d - 1 + 1 = d$ pairwise linearly independent directions perpendicular to σ . Let S^* be a minimal subset of directions in S satisfying the conditions of perpendicularity and one-dimensional envelopes.

We bound the size of S^* by considering how such a set could be constructed. Naïvely, for each edge σ , we could choose d pairwise linearly independent directions perpendicular to σ , so that we would have $|S^*| = n_1 d$. However, this is generally more directions than we need; collections of $m < d$ edges are all parallel to a common m -plane (the plane spanned by the edges if they are considered as vectors), so a single direction may be perpendicular to many edges at once. Also note that d pairwise linearly independent directions all perpendicular to an edge do not necessarily define a one-dimensional envelope. The challenge then, is to find the minimum number of directions in S^* so that all envelopes are one-dimensional, while noting that some directions may be perpendicular to multiple edges at a time.

We construct S^* as follows. First, note that the edges of K are all contained in a common n_1 -plane, so there is a $(d - n_1 - 1)$ -sphere's worth of directions perpendicular to *all* edges simultaneously. Since $d - n_1 - 1 > 0$, there are uncountably infinite such directions; they are maximally efficient in the sense that a single direction can “count” for all edges at once. Choose any $d - 1$ pairwise linearly independent directions from this sphere to be included in the set S^* . So far, each edge only has $d - 1$ directions perpendicular to it; we need an additional perpendicular direction for each edge to bring the total for each edge up to d . However, in order to ensure the envelopes of each edge are one-dimensional, these additional directions must not be perpendicular to any hyperplane defined by subsets of more than one edge. This means we must consider a total of n_1 additional directions, so that S^* has cardinality $d - 1 + n_1$. Since $|S^*|$ lower bounds $|S|$, we find $|S| \in \Omega(d + n_1)$. \square

Remark 2 (Why Bound n_1 ?). *Bounding the number of edges for our construction in the proof of Theorem 2 may seem counterintuitive. It feels natural to suppose more edges require more directions. However, in the asymptotic analysis, we see this increased need for directions that are perpendicular to each edge being balanced by the increase of subsets of edges that are parallel to common $(d-1)$ -planes, and the increasing ability of a single direction to contribute to the totals for multiple edges at once.*

To construct S^ if $n_1 \geq d-1$, we could choose directions simultaneously perpendicular to sets of $d-1$ edges, choosing the sets so the envelopes of each edge are one-dimensional. In order to ensure each edge has d directions perpendicular to it, we perform this near-partition of the total edge set d times, so the asymptotic size of S^* is (surprisingly), $d \left\lceil \frac{n_1}{d-1} \right\rceil \in \Omega(n_1)$. In particular, the increased presence of subsets of edges parallel to the same hyperplane yields an asymptotic lower bound that is independent of d .*

6.2 Verbose Descriptor Bounds

We now shift to verbose descriptors, and begin with the tight lower bound.

Lemma 11 (Tight Lower Bound). *Let K be a simplicial complex in \mathbb{R}^d and let $\hat{D} \in \{\hat{\chi}, \hat{\beta}, \hat{\rho}\}$. Suppose that $\hat{D}(K, S)$ is faithful. Then $|S| \geq d$, and this bound is tight.*

Proof. No vertex in K can be described using fewer than d coordinates. Thus, a set of descriptors of type \hat{D} with cardinality less than d cannot be faithful for K_0 , let alone K . To see that this bound is tight, consider the case where K is a single vertex; verbose descriptors generated by any d pairwise linearly independent directions form a faithful set for the vertex (e.g., $\hat{D}(K, \{e_1, e_2, \dots, e_d\})$). \square

In many examples, we find that minimum faithful sets of verbose descriptors for simple simplicial complexes in \mathbb{R}^d often have cardinality $d+1$. Independence from the size of the simplicial complex is not too surprising, since verbose descriptors always have events corresponding to each simplex.

In the remainder of this section, we identify a family of simplicial complexes for which minimal faithful sets of verbose persistence diagrams (and by reduction, also verbose Betti functions and verbose Euler characteristic curves) are linear in the number of vertices. We use $\alpha_{i,j}$ to denote the angle that vector $v_j - v_i$ makes with the x -axis. We assume all angles take value in $[0, 2\pi)$. We establish a preliminary observation, a specific instance of the general phenomenon that a simplicial complex stratifies the sphere of directions based on vertex order [3, 44].

Observation 1. *Suppose that a simplicial complex K in \mathbb{R}^2 contains an edge $[v_1, v_2]$ such that v_1 and v_2 have degree one. Then a birth event occurs at the height of v_1 in $\hat{\rho}(K, s)$ for all s in the half of \mathbb{S}^1 defined by the open interval $I = (\alpha_{1,2} - \pi, \alpha_{1,2} + \pi)$ (i.e., all s so that $s \cdot v_1 > s \cdot v_2$) and as an instantaneous event for $s \in I^C$ (i.e., all s so that $s \cdot v_1 \leq s \cdot v_2$).*

We also establish the following lemma.

Lemma 12. *Consider a pair of nested triangles as in Figure 9. Then angle A is larger than θ , $\phi - B$, and $\psi - C$.*

Proof. Adding angles in the larger triangle, we see $\theta + \phi + \psi = \pi$. Then,

$$\begin{aligned} \theta + (\phi - B) + B + (\psi - C) + C &= \pi \\ A + \theta + (\phi - B) + B + (\psi - C) + C &= A + \pi \\ (A + B + C) + \theta + (\phi - B) + (\psi - C) &= A + \pi \\ \pi + \theta + (\phi - B) + (\psi - C) &= A + \pi \\ \theta + (\phi - B) + (\psi - C) &= A. \end{aligned}$$

All the terms in the last line are positive, meaning A is larger than θ , $\phi - B$, and $\psi - C$. \square

We now construct the building block that forms the complexes used in our bound.

Construction 1 (Clothespin Motif). *Let K be a simplicial complex in \mathbb{R}^2 with a vertex set $\{v_1, v_2, v_3, v_4\}$. Suppose that only v_3 is in the interior of the convex hull of $\{v_1, v_2, v_4\}$, and that the edge set consists of $[v_1, v_2]$ and $[v_3, v_4]$. See Figure 10a.*

Construction 1 was built specifically for the following necessary condition for faithful sets of verbose descriptors. We state this condition in terms of $\hat{\rho}$'s in the following lemma.

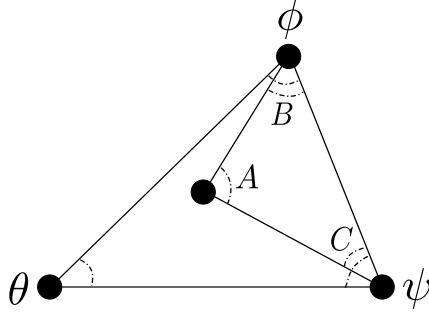


Figure 9: Nested triangles as discussed in Lemma 12

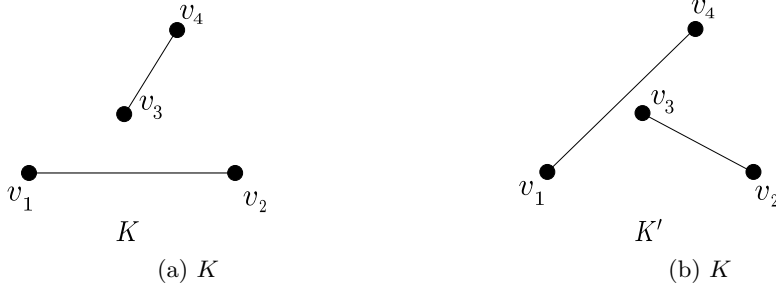


Figure 10: The two simplicial complexes considered in the proof of Lemma 13.

Lemma 13 (Clothespin Representability). *Let K be a clothespin motif, as in Construction 1, and suppose that $\hat{\rho}(K, S)$ is faithful. Then we have at least one direction $s \in S$ such that the angle formed between s and e_1 lies in the region $[\alpha_{3,2} - \pi, \alpha_{3,4} - \pi] \cup [\alpha_{3,2} + \pi, \alpha_{3,4} + \pi]$.*

Proof. Let K' be a simplicial complex in \mathbb{R}^2 with the same vertex set as K , but with edges $[v_1, v_4]$ and $[v_2, v_3]$ (see Figure 10b). Recall that, since $\hat{\rho}(K, S)$ is faithful, by definition, the set S must contain some direction s so that $\hat{\rho}(K, s) \neq \hat{\rho}(K', s)$.

Each vertex corresponds to either a birth event or an instantaneous event depending on the direction of filtration. We proceed by considering each vertex v_i individually and determining subsets $R_i \subset \mathbb{S}^1$ such that, whenever $s \in R_i$, the event at $s \cdot v_i$ is different when filtering over K versus K' , but for $s_* \notin R_i$, the type of event at $s_* \cdot v_i$ is the same between the two graphs. Figure 11 shows these regions, and in what follows, we define them precisely.

First, consider v_1 . By Observation 1, $v_1 \in K$ corresponds to a birth event for all directions in the interval $B = (\alpha_{1,2} - \pi, \alpha_{1,2} + \pi)$ and $v_1 \in K'$ corresponds to a birth event for all directions in the interval $B' = (\alpha_{1,4} - \pi, \alpha_{1,4} + \pi)$. Then we write $R_1 = (B \setminus B') \cup (B' \setminus B)$, which is the wedge-shaped region such that for any $s \in R_1$, the type of event associated to $v_1 \in K$ and $v_1 \in K'$ differ, meaning $\hat{\rho}(K, s) \neq \hat{\rho}(K', s)$.

Using this same notation, identify the wedge shaped region R_i for vertex $i \in [2, 3, 4]$ such that any direction from R_i generates $\hat{\rho}$'s that have different event types at vertex v_i when filtering over K versus K' . Similar arguments for $i \in [2, 3, 4]$ give us the complete list;

$$\begin{aligned} R_1 &= (\alpha_{1,2} - \pi, \alpha_{1,4} - \pi] \cup [\alpha_{1,2} + \pi, \alpha_{1,4} + \pi) \\ R_2 &= (\alpha_{2,3} - \pi, \alpha_{2,1} - \pi] \cup [\alpha_{2,3} + \pi, \alpha_{2,1} + \pi) \\ R_3 &= (\alpha_{3,2} - \pi, \alpha_{3,4} - \pi] \cup [\alpha_{3,2} + \pi, \alpha_{3,4} + \pi) \\ R_4 &= (\alpha_{1,4} - \pi, \alpha_{3,4} - \pi] \cup [\alpha_{1,4} + \pi, \alpha_{3,4} + \pi) \end{aligned}$$

Let $W = \bigcup_{i=1}^4 R_i$. Then, for any $s \in W$, we have $\hat{\rho}(K, s) \neq \hat{\rho}(K', s)$, and for any $s_* \in W^C$, we have $\hat{\rho}(K, s_*) = \hat{\rho}(K', s_*)$.

Finally, we claim that W is the closure of R_3 , denoted $\overline{R_3}$, i.e., exactly the region described in the lemma statement. This is a direct corollary to Lemma 12; the angles swept out by each regions correspond to the angles formed by pairs of edges in K and K' ; in particular, the angle $\angle v_2 v_3 v_4$ is the largest and geometrically contains the others. This means the extremal boundaries over all R_i 's are formed by the angles $\alpha_{2,3} \pm \pi$ and $\alpha_{3,4} \pm \pi$, the defining angles of R_3 . Each of these four angles appears as an included endpoint for some R_i , so $R_1, R_2, R_4 \subseteq \overline{R_3} = W$ (Figure 11) and we have shown our claim. \square

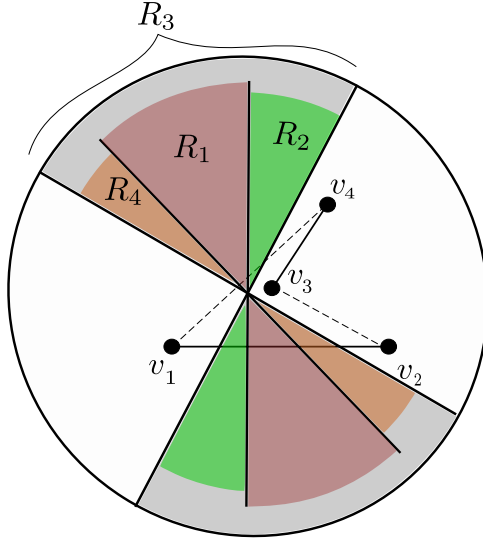


Figure 11: The regions described in the proof of Lemma 13, with additional shading in the interior of the sphere of directions to aid in visibility. K is shown as solid black edges and K' as dashed edges. For any lower-star filtration in a direction contained in R_i , the event at vertex v_i differs when considering K or K' , thus, such directions are able to distinguish K from K' . Note that any direction outside the regions of observability (i.e., the non-shaded portions of the circle) is not able to distinguish K from K' .

We refer to the two antipodal intervals of directions in \mathbb{S}^1 for which the corresponding verbose diagrams have this distinction as a clothespin's *region of observability* (similar to observability for χ 's discussed in [3, 41]). We notate the region as $W = [\alpha_{3,4} - \pi, \alpha_{2,3} - \pi] \cup [\alpha_{3,4} + \pi, \alpha_{2,3} + \pi]$. Crucially, W is defined by the angle $\angle v_2 v_3 v_4$, so a different embedding of K could result in a smaller region.

Remark 3 (W Can be Arbitrarily Small). *As the angle $\angle v_2 v_3 v_4$ approaches zero, the region of observability, W , described in the proof of Lemma 13 also approaches zero.*

To construct a family of simplicial complexes, each of which must have at least $\Theta(n_0)$ verbose descriptors to form a faithful set, we use Remark 3 to knit together clothespin motifs (Construction 1):

Construction 2 (Clothespins on a Semicircular Clothesline). *Let K_m be a simplicial complex in \mathbb{R}^2 formed by m copies of Construction 1 (m clothespin motifs) such that the regions of observability for each clothespin do not intersect. Note this is possible for any m by Remark 3.*

See Figure 12 for an example of K_m for $m = 4$. This construction implies a lower bound on the number of $\hat{\rho}$'s needed to fully represent a simplicial complex.

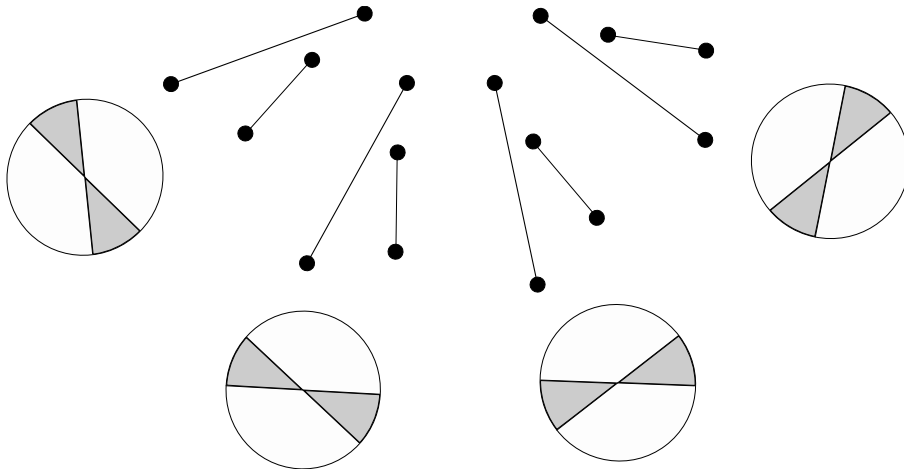


Figure 12: An example of Construction 2 for $m = 4$. The regions of observability are shown below each clothespin. By construction, each of these four double wedges define disjoint regions of \mathbb{S}^2 .

Lemma 14 (Lower Bound for Worst-Case $\hat{\rho}$'s Complexity). *Let K_m be as in Construction 2 and suppose $\hat{\rho}(K_m, S)$ is a faithful set. Then S must contain at least one direction in each of the m regions of observability, meaning that $|S| \geq m = n_0/4$. Thus, the size of a faithful set of $\hat{\rho}$'s for K_m is $\Omega(n_0)$.*

Note that by Theorem 1, the above lemma implies the following theorem.

Theorem 3 (Lower Bound for Worst-Case Verbose Descriptor Complexity). *Let $\hat{D} \in \{\hat{\chi}, \hat{\beta}, \hat{\rho}\}$. Then the worst-case cardinality of a minimal descriptor set of type \hat{D} is $\Omega(n_0)$.*

7 Discussion

In this paper, we provide a framework for comparing abstract topological descriptors by their ability to represent simplicial complexes. This framework is constructed to allow for the analysis of general topological descriptor types, and the theory developed here makes it possible for more rigorous theoretical justifications of choosing a particular descriptor type for use in applications.

We focus on six topological descriptors that are particularly relevant to applications and related work; verbose and concise Euler characteristic functions, verbose and concise Betti functions, and verbose and concise persistence diagrams. We give a partial order on this set of six descriptors, including the strict inequality, $[\hat{\beta}] \prec [\hat{\rho}]$.

We then identify tight lower bounds for both concise and verbose descriptors in the set of six, as well as asymptotic lower bounds for worst-case complexity of the concise and verbose descriptors. The lower bounds for worst-case complexity quantify the observation that the concise descriptors in our set of six are much weaker than the verbose descriptors, as they require many perpendicular directions to each maximal simplex. Since verbose descriptors have events at the height of each vertex, one might suppose (and find to be generally true) that the size of a faithful set of verbose descriptors only depends on the ambient dimension. We find an unexpected construction that requires a faithful set of verbose descriptors to have size linear in the number of vertices.

Perhaps the strength classes $[\beta]$, $[\chi]$, and $[\rho]$ intuitively feel as though they should be related by strict inequalities. However, the issue of verifying non-equality or equality between concise strength classes is nuanced. We know by Lemma 16 (Appendix A) that general position assumptions can have an impact on this set. But even after taking general position assumptions, the seemingly advantageous ‘‘extra’’ information of homology compared to Betti numbers or Euler characteristic is perhaps no longer so advantageous when faithful sets already need to make tight envelopes around each maximal simplex. That is, once we have all the (many) required directions, we have already carved out the space filled by the complex, and already know quite a lot simply from the presence of events. Non-equality or equality of concise descriptors remains as an area active of research.

In other ongoing work, we hope to classify the simplicial complexes for which minimal faithful sets of verbose descriptors are independent of the size of the complex. We are also interested in relating other common descriptor types, such as merge trees.

References

- [1] Katharine Turner, Sayan Mukherjee, and Doug M. Boyer. Persistent homology transform for modeling shapes and surfaces. *Information and Inference: A Journal of the IMA*, 3(4):310–344, 2014.
- [2] Robin Lynne Belton, Brittany Terese Fasy, Rostik Mertz, Samuel Micka, David L. Millman, Daniel Salinas, Anna Schenfisch, Jordan Schupbach, and Lucia Williams. Reconstructing embedded graphs from persistence diagrams. *Computational Geometry: Theory and Applications*, 90, October 2020.
- [3] Justin Curry, Sayan Mukherjee, and Katharine Turner. How many directions determine a shape and other sufficiency results for two topological transforms. *Transactions of the American Mathematical Society, Series B*, 9(32):1006–1043, 2022.
- [4] Brittany Terese Fasy, Samuel Micka, David L. Millman, Anna Schenfisch, and Lucia Williams. Efficient graph reconstruction and representation using augmented persistence diagrams. *Proceedings of the 34th Annual Canadian Conference on Computational Geometry*, 2022.
- [5] Samuel Micka. *Algorithms to Find Topological Descriptors for Shape Reconstruction and How to Search Them*. PhD thesis, Montana State University, 2020.

- [6] Yongjin Lee, Senja D. Barthel, Paweł Dłotko, S. Mohamad Moosavi, Kathryn Hess, and Berend Smit. Quantifying similarity of pore-geometry in nanoporous materials. *Nature Communications*, 8:15396, 2017.
- [7] Abbas H. Rizvi, Pablo G. Camara, Elena K. Kandror, Thomas J. Roberts, Ira Schieren, Tom Maniatis, and Raul Rabadan. Single-cell topological RNA-seq analysis reveals insights into cellular differentiation and development. *Nature Biotechnology*, 35(6):551, 2017.
- [8] Peter Lawson, Jordan Schupbach, Brittany Terese Fasy, and John W. Sheppard. Persistent homology for the automatic classification of prostate cancer aggressiveness in histopathology images. In *Medical Imaging 2019: Digital Pathology*, volume 10956, page 109560G. International Society for Optics and Photonics, 2019.
- [9] Sarah Tymochko, Elizabeth Munch, Jason Dunion, Kristen Corbosiero, and Ryan Torn. Using persistent homology to quantify a diurnal cycle in hurricanes. *Pattern Recognition Letters*, 2020.
- [10] Yuan Wang, Hernando Ombao, and Moo K Chung. Statistical persistent homology of brain signals. In *IEEE International Conference on Acoustics, Speech and Signal Processing (ICASSP)*, pages 1125–1129, 2019.
- [11] Paul Bendich, James S. Marron, Ezra Miller, Alex Pieloch, and Sean Skwerer. Persistent homology analysis of brain artery trees. *The Annals of Applied Statistics*, 10(1):198, 2016.
- [12] Qitong Jiang, Sebastian Kurtek, and Tom Needham. The weighted Euler curve transform for shape and image analysis. In *Proceedings of the IEEE/CVF Conference on Computer Vision and Pattern Recognition Workshops*, pages 844–845, 2020.
- [13] Erik J. Amézquita, Michelle Y. Quigley, Tim Ophelders, Jacob B. Landis, Daniel Koenig, Elizabeth Munch, and Daniel H. Chitwood. Measuring hidden phenotype: Quantifying the shape of barley seeds using the Euler characteristic transform. *in silico Plants*, 4(1):diab033, 2022.
- [14] Kalyan Varma Nadimpalli, Amit Chattopadhyay, and Bastian Rieck. Euler characteristic transform based topological loss for reconstructing 3D images from single 2D slices. In *Proceedings of the IEEE/CVF Conference on Computer Vision and Pattern Recognition*, pages 571–579, 2023.
- [15] Eitan Richardson and Michael Werman. Efficient classification using the euler characteristic. *Pattern Recognition Letters*, 49:99–106, 2014.
- [16] Lorin Crawford, Anthea Monod, Andrew X. Chen, Sayan Mukherjee, and Raúl Rabadán. Predicting clinical outcomes in glioblastoma: an application of topological and functional data analysis. *Journal of the American Statistical Association*, 115(531):1139–1150, 2020.
- [17] Kun Meng, Jinyu Wang, Lorin Crawford, and Ani Eloyan. Randomness and statistical inference of shapes via the smooth Euler characteristic transform, 2022. arXiv:2204.12699.
- [18] Lewis Marsh and David Beers. Stability and inference of the Euler characteristic transform, 2023. arXiv:2303.13200.
- [19] Ameer Saadat-Yazdi, Rayna Andreeva, and Rik Sarkar. Topological detection of alzheimer’s disease using Betti curves. In *Interpretability of Machine Intelligence in Medical Image Computing, and TDA and Its Applications for Medical Data.*, pages 119–128. Springer, 2021.
- [20] Jianyang Li, Lei Yang, Yunan He, and Osamu Fukuda. Classification of hand movements based on EMG signals using topological features. *International Journal of Advanced Computer Science and Applications*, 14(4), 2023.
- [21] Patrizio Frosini and Claudia Landi. Persistent Betti numbers for a noise tolerant shape-based approach to image retrieval. *Pattern Recognition Letters*, 34(8):863–872, 2013.
- [22] Pratyush Pranav, Herbert Edelsbrunner, Rien Van de Weygaert, Gert Vegter, Michael Kerber, Bernard JT Jones, and Mathijs Wintraecken. The topology of the cosmic web in terms of persistent Betti numbers. *Monthly Notices of the Royal Astronomical Society*, 465(4):4281–4310, 2017.

- [23] Georg Wilding, Keimpe Nevenzeel, Rien van de Weygaert, Gert Vegter, Pratyush Pranav, Bernard JT Jones, Konstantinos Efstathiou, and Job Feldbrugge. Persistent homology of the cosmic web—I. hierarchical topology in λ CDM cosmologies. *Monthly Notices of the Royal Astronomical Society*, 507(2):2968–2990, 2021.
- [24] Rien Van De Weygaert, Erwin Platen, Gert Vegter, Bob Eldering, and Nico Kruithof. Alpha shape topology of the cosmic web. In *2010 International Symposium on Voronoi Diagrams in Science and Engineering*, pages 224–234. IEEE, 2010.
- [25] Chad Giusti, Eva Pastalkova, Carina Curto, and Vladimir Itskov. Clique topology reveals intrinsic geometric structure in neural correlations. *Proceedings of the National Academy of Sciences*, 112(44):13455–13460, 2015.
- [26] Gurjeet Singh, Facundo Mémoli, and Gunnar E. Carlsson. Topological methods for the analysis of high dimensional data sets and 3D object recognition. *SPBG*, 91:100, 2007.
- [27] Levent Batakci, Abigail Branson, Bryan Castillo, Candace Todd, Erin Wolf Chambers, and Elizabeth Munch. Comparing embedded graphs using average branching distance. *Involve, a Journal of Mathematics*, 16(3):365–388, 2023.
- [28] Allen Hatcher. Algebraic topology, Cambridge Univ. Press, Cambridge, 2002.
- [29] Herbert Edelsbrunner and John Harer. *Computational Topology: An Introduction*. American Mathematical Society, 2010.
- [30] Alexander McCleary and Amit Patel. Edit distance and persistence diagrams over lattices. *SIAM Journal on Applied Algebra and Geometry*, 6(2):134–155, 2022.
- [31] Brittany Terese Fasy and Amit Patel. Persistent homology transform cosheaf, 2022.
- [32] Alexander McCleary and Amit Patel. Edit distance and persistence diagrams over lattices. *SIAM Journal on Applied Algebra and Geometry*, 6(2):134–155, 2022.
- [33] Michael Usher and Jun Zhang. Persistent homology and Floer–Novikov theory. *Geometry & Topology*, 20(6):3333–3430, 2016.
- [34] Wojciech Chachólski, Barbara Giunti, Alvin Jin, and Claudia Landi. Decomposing filtered chain complexes: Geometry behind barcoding algorithms. *Computational Geometry*, 109:101938, 2023.
- [35] Facundo Mémoli and Ling Zhou. Stability of filtered chain complexes, 2022. arXiv:2208.11770.
- [36] Facundo Mémoli and Ling Zhou. Ephemeral persistence features and the stability of filtered chain complexes. In *39th International Symposium on Computational Geometry (SoCG 2023)*. Schloss Dagstuhl-Leibniz-Zentrum für Informatik, 2023.
- [37] Ling Zhou. *Beyond Persistent Homology: More Discriminative Persistent Invariants*. PhD thesis, The Ohio State University, 2023.
- [38] Brittany Terese Fasy, Samuel Micka, David L. Millman, Anna Schenfisch, and Lucia Williams. Challenges in reconstructing shapes from Euler characteristic curves, 2018. arXiv:1811.11337.
- [39] Zhen Zhou, Yongzhen Huang, Liang Wang, and Tieniu Tan. Exploring generalized shape analysis by topological representations. *Pattern Recognition Letters*, 87:177–185, 2017.
- [40] Thomas Jech. Set theory. *Journal of Symbolic Logic*, pages 876–77, 1981.
- [41] Brittany Terese Fasy, Samuel Micka, David L. Millman, Anna Schenfisch, and Lucia Williams. Challenges in reconstructing shapes from Euler characteristic curves. *Fall Workshop Computational Geometry*, 2018.
- [42] J. Darrotto. Convex optimization and Euclidean distance geometry. *Palo Alto: Meboo*, 2013.
- [43] Michael J. Panik. *Fundamentals of convex analysis: duality, separation, representation, and resolution*, volume 24. Springer Science & Business Media, 2013.
- [44] Jacob Leygonie, Steve Oudot, and Ulrike Tillmann. A framework for differential calculus on persistence barcodes. *Foundations of Computational Mathematics*, pages 1–63, 2021.

A Zoo of Other Descriptor Types

In Section 2, we adopt a general definition of topological descriptor (Definition 1). In this appendix, we explore non-standard topological descriptors, and corresponding scenarios that may arise as a result of this generality. The descriptors presented here are not intended to be taken as anything that would necessarily make sense to use in practice, but rather, as a sort of zoo of examples to get a quick glance at the mathematical extremes and properties of the space of strength classes of topological descriptors.

First, we observe that many examples of topological descriptors are not capable of faithfully representing most simplicial complexes (even simplicial complexes satisfying strict general position assumptions), such as the following.

Example 1 (Descriptor Type Only Faithful for Convex Point Clouds). *Consider a descriptor that returns (1) the coordinates of the lowest vertex (or vertices) in a lower-star filtration and (2) the cardinality of the vertex set, but no other information. Any set of vertices that defines the corners of a convex region can be faithfully represented by this descriptor, but this descriptor type is incapable of faithfully representing any other type of simplicial complex.*

We can also construct descriptor types that are simply never able to form faithful sets.

Example 2 (Descriptor Incapable of Faithfully Representing Any Complex). *Consider the trivial descriptor type that returns zero for all sublevel sets in a lower-star filtration. Although it is an invariant of the filtration, it can not faithfully represent any simplicial complex.*

Thus, in the space of all topological descriptors, the trivial descriptor of Example 2 is in the minimum strength class. We can (also trivially) construct a descriptor type that is in the maximum strength class.

Example 3 (Faithful Sets of Size One). *Consider the trivial descriptor type that returns all sublevel sets in a lower-star filtration. Thus, a single descriptor of this type is always faithful for a simplicial complex.*

Finally, we can find instances of topological descriptors that are able to faithfully represent a simplicial complex, but with a set no smaller than uncountably infinite.

Example 4 (Descriptor with Uncountable Minimum Faithful Sets). *Let K be a simplicial complex in \mathbb{R}^d let D be a descriptor type parameterized by \mathbb{R}^d that is constant over a filtration and is defined by*

$$D(K, (x_1, x_2, \dots, x_d)) = \begin{cases} 1 & \text{if } K \cap (x_1, x_2, \dots, x_d) \neq \emptyset \\ 0 & \text{else.} \end{cases}$$

Then $D(K, \mathbb{R}^d)$ is the minimum faithful set for K .

Thus, the (minimal) strength class of the descriptor in Example 4 is greater than the strength class of the trivial descriptor in Example 3, and there are no strength equivalence classes between them.

We now know the space of strength classes of topological descriptors has a minimum and maximum, and we have identified a second smallest descriptor type; is it a total order? The following example shows that it is not; there do indeed exist incomparable descriptor types.

Lemma 15 (Incomparable Strength Classes). *There exist incomparable strength classes of topological descriptor types.*

Proof. Let D be the descriptor type of Example 1. That is, given a direction s , D returns: (1) the coordinates of the lowest vertex (or vertices) in a lower-star filtration in direction s , and (2) the cardinality of the vertex set. We compare D with $\hat{\rho}$. Let $v_1 = (0, 0)$ and $v_2 = (0, 1)$.

First, consider the simplicial complex $K = [v_1]$. Then, regardless of direction, a single descriptor of is faithful for K . However, since K is in \mathbb{R}^2 , any faithful set of $\hat{\rho}$'s must have at least two linearly independent directions to recover both coordinates of K .

Next, consider the simplicial complex $K' = [v_1, v_2]$. No set of descriptors of type D is faithful for K' (it cannot distinguish between K' and the simplicial complex consisting of the two disconnected vertices v_1 and v_2 without an edge). However, two $\hat{\rho}$'s suffice to form a faithful set for K' ; for example, the set $\hat{\rho}(K', \{e_1, e_2\})$. Thus, if $D(K, S_D)$ and $\hat{\rho}(K, S_{\hat{\rho}})$ are both minimal faithful sets, we see that $|S_D| < |S_{\hat{\rho}}|$ but $|S_D| > |S_{\hat{\rho}}|$. Thus, although we have shown $[D] \neq [\hat{\rho}]$, they are incomparable. \square

Finally, we give a lemma that shows an impact of not adopting any general position assumptions.

Lemma 16 (Concise Equality). *Without general position assumptions, the strength equivalence classes of χ , β , and ρ are all equal.*

Proof. We must consider faithful sets of such descriptors for an arbitrary simplicial complex K . The argument differs depending on if K is a vertex set, or contains at least one edge; we consider each case.

First, consider faithful sets for simplicial complexes K in \mathbb{R}^d with $n_1 = 0$; since K is a vertex set, all maximal simplices are vertices, so all envelopes must be zero-dimensional by Lemma 10. Then, by Corollary 1, faithful sets of χ 's, β 's, or ρ 's must include descriptors from at least $d + 1$ pairwise linearly independent directions. Notice the envelope of each vertex contains that vertex and nothing else. That is, we know the exact location of each vertex by identifying its envelope. Thus, minimal faithful sets of χ 's, β 's, or ρ 's have cardinality of exactly $d + 1$.

Next, consider faithful sets for complexes K with $n_1 > 1$. We show no set of $D \in \{\chi, \beta, \rho\}$ can faithfully represent such a K . Let K' be identical to K , but with the simplices subdivided into a finer set of simplices. Then for every direction s , $D(K, s) = D(K', s)$. Since this is true for every s , the descriptor types χ , β , and ρ are incapable of forming faithful sets for such simplicial complexes, and thus are of equal strength equivalence classes. Considering both cases, we find $[\chi] = [\beta] = [\rho]$. \square